Sintering of Catalytic Nanoparticles: Particle Migration or Ostwald Ripening?

THOMAS W. HANSEN,[†] ANDREW T. DELARIVA,[‡]
SIVAKUMAR R. CHALLA,[‡] AND ABHAYA K. DATYE*,[‡]

[†]Center for Electron Nanoscopy, Technical University of Denmark, DK-2800 Kgs.
Lyngby, Denmark, and [‡]Department of Chemical & Nuclear Engineering and
Center for Microengineered Materials, MSC 01 1120, University of New Mexico,
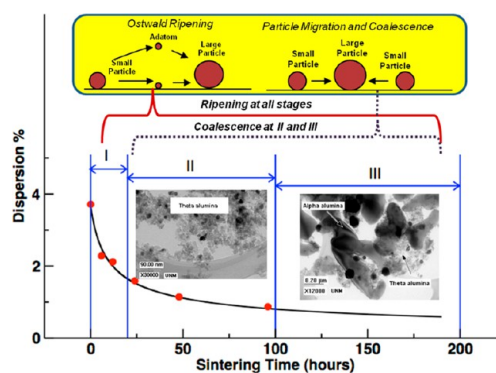Albuquerque, New Mexico 87131-0001, United States

CONSPECTUS

Metal nanoparticles contain the active sites in heterogeneous catalysts, which are important for many industrial applications including the production of clean fuels, chemicals and pharmaceuticals, and the cleanup of exhaust from automobiles and stationary power plants. Sintering, or thermal deactivation, is an important mechanism for the loss of catalyst activity. This is especially true for high temperature catalytic processes, such as steam reforming, automotive exhaust treatment, or catalytic combustion. With dwindling supplies of precious metals and increasing demand, fundamental understanding of catalyst sintering is very important for achieving clean energy and a clean environment, and for efficient chemical conversion processes with atom selectivity.

Scientists have proposed two mechanisms for sintering of nanoparticles: particle migration and coalescence (PMC) and Ostwald ripening (OR). PMC involves the mobility of particles in a Brownian-like motion on the support surface, with subsequent coalescence leading to nanoparticle growth. In contrast, OR involves the migration of adatoms or mobile molecular species, driven by differences in free energy and local adatom concentrations on the support surface.

In this Account, we divide the process of sintering into three phases. Phase I involves rapid loss in catalyst activity (or surface area), phase II is where sintering slows down, and phase III is where the catalyst may reach a stable performance. Much of the previous work is based on inferences from catalysts that were observed before and after long term treatments. While the general phenomena can be captured correctly, the mechanisms cannot be determined. Advancements in the techniques of in situ TEM allow us to observe catalysts at elevated temperatures under working conditions. We review recent evidence obtained via in situ methods to determine the relative importance of PMC and OR in each of these phases of catalyst sintering. The evidence suggests that, in phase I, OR is responsible for the rapid loss of activity that occurs when particles are very small. Surprisingly, very little PMC is observed in this phase. Instead, the rapid loss of activity is caused by the disappearance of the smallest particles. These findings are in good agreement with representative atomistic simulations of sintering. In phase II, sintering slows down since the smallest particles have disappeared. We now see a combination of PMC and OR, but do not fully understand the relative contribution of each of these processes to the overall rates of sintering. In phase III, the particles have grown large and other parasitic phenomena, such as support restructuring, can become important, especially at high temperatures. Examining the evolution of particle size and surface area with time, we do not see a stable or equilibrium state, especially for catalysts operating at elevated temperatures.

In conclusion, the recent literature, especially on in situ studies, shows that OR is the dominant process causing the growth of nanoparticle size. Consequently, this leads to the loss of surface area and activity. While particle migration could be controlled through suitable structuring of catalyst supports, it is more difficult to control the mobility of atomically dispersed species. These insights into the mechanisms of sintering could help to develop sinter-resistant catalysts, with the ultimate goal of designing catalysts that are self-healing.

Introduction

Metal nanoparticles constitute the active sites in heterogeneous catalysts, which are important for many industrial applications including the production of clean fuels, chemicals, and pharmaceuticals and in cleanup of exhaust from automobiles and stationary power plants. In the catalysis
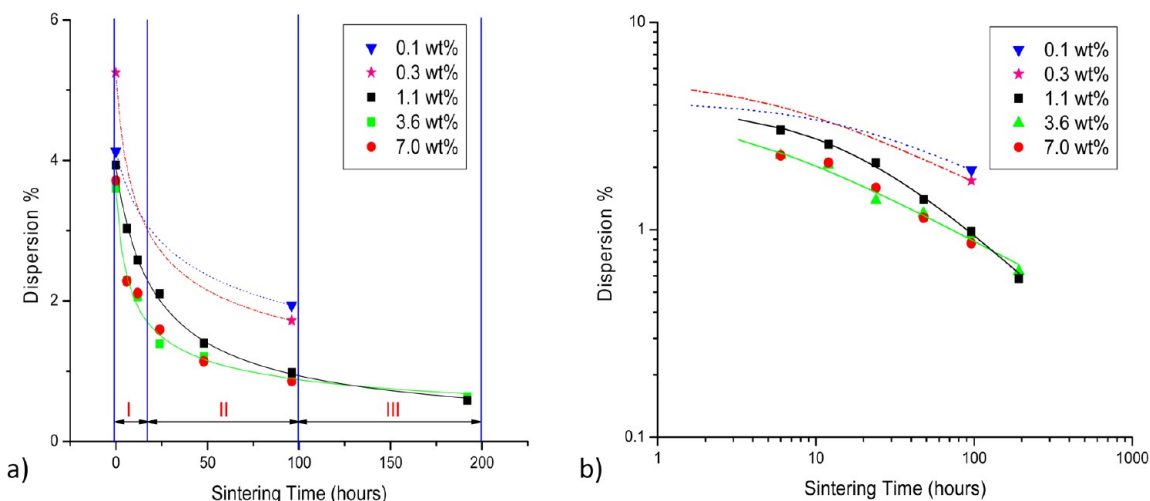
FIGURE 1. Evolution of catalyst dispersion for Pd/alumina as a function of time when heated at 900 °C in flowing 10% H_2O/N_2 plotted on a (a) linear and (b) logarithmic scale. On the linear scale, catalyst dispersion decays rapidly in phase I, then seems to stabilize (phase II) and appears to reach an equilibrium dispersion (phase III). The data are fit to the eq $1/D^n = 1/D_0^n + kt$ where D is the catalyst dispersion at time t, D_0 is the dispersion at time = 0, and n is a power law exponent (Reprinted from Xu et al.,[28] *ChemCatChem*, with permission).

literature, the growth of supported metal nanoparticles is referred to as *sintering* and it results in loss of active surface area. Sintering, or thermal deactivation, is an important mechanism for the loss of catalyst activity, especially for high temperature catalytic processes, such as steam reforming and automotive exhaust conversion. With dwindling supplies of precious metals and increasing demand, fundamental understanding of catalyst sintering is of paramount importance for achieving societal goals of clean energy, a clean environment, and atom selectivity in chemical conversion processes.

A catalyst containing a low loading of metal will initially contain small metal particles, generally less than 2 nm in size. When such a catalyst is used in a reaction environment, we see a growth in the size of the nanoparticles, a process termed sintering. The growth of nanoparticles can be understood in terms of two operative mechanisms: Ostwald ripening (OR) or particle migration and coalescence (PMC). Ripening involves interparticle transport of mobile species, with larger particles growing at the expense of smaller particles due to differences in surface energy. Particle migration involves the Brownian motion of nanoparticles leading to coalescence when particles come in close proximity to each other. Previous literature[1,2] has suggested that the operative mechanism may change from particle migration, in the early stages when the nanoparticles are very small, to Ostwald ripening, when the particles become large and effectively immobile. Two approaches were used to deduce mechanisms of catalyst sintering. One approach was based on the observed particle size distributions (PSD) in the

sintered catalysts.[3] It was suggested by Granqvist and Buhrman[3] that PMC would lead to a log-normal size distribution with a long tail toward the larger particle sizes. On the other hand, OR would lead to a distribution with a tail toward the smaller particles, and a cutoff in the size distribution at a particle diameter generally 1.3−1.5 times the mean diameter.[2] Since most published PSDs from heterogeneous catalysts can be fit to a log-normal distribution, it is questionable whether mechanisms can be determined using this approach.[4] Furthermore, it has also been suggested that OR could lead to a PSD that is similar to a log-normal distribution.[5]

The second approach for determining mechanisms of sintering was based on the growth kinetics, that is, the change in average particle size as a function of time.[2] Changes in the slope of this curve were used to infer changes in the mechanism. However, it is not clear that these changes in slope have mechanistic significance since the observed exponent depends on the time frame of observation. The change in slope is illustrated by reference to a plot of catalyst surface area (or dispersion, number of surface atoms divided by the total number of atoms) as a function of time. Figure 1 shows results for the sintering of Pd/Al$_2$O$_3$ treated isothermally in a 10%H$_2$O/N$_2$ atmosphere to simulate automotive exhaust. The dispersion shows a rapid decrease with time, followed by a more gradual change. Sintering is rapid at first and then slows down. To help understand the fundamental mechanistic aspects, we propose to divide the process of catalyst sintering into three distinct phases.

Three Phases of Catalyst Sintering. The distinction into these three phases is qualitative, and the specific time for the transition from one phase to another depends on the metal, support, and gas atmosphere. This report seeks to answer some specific questions that are most relevant to each phase. Phase I: Is the rapid decay in activity in the early stage of sintering caused by migration and coalescence of particles? Phase II: Why does sintering slow down? Phase III: Do catalysts reach a stable, equilibrium dispersion (or particle size)? These three phases also pertain to specific size ranges for metal nanoparticles. When particles are very small (diameter $d < 3$ nm), they are expected to be mobile, and this could be a possible explanation for the rapid sintering seen in phase I. As particles grow in size, they become more stable ($3 < d < 10$ nm) and sintering slows down, as in phase II. In the later stages, particles can grow quite large ($d > 10$ nm) and they are most likely immobile, suggesting that atom transfer is the most likely mechanism. Other parasitic phenomena such as loss of support surface area and phase transformations of the support become important in phase III.

Nanoparticle Mobility. According to classical theory, adatom diffusion on the surface of a metal nanoparticle can cause the center of mass of the nanoparticle to move. The collective result from the diffusion of surface atoms over time can result in a diffusive particle migration.[2] Models relating the diffusion of a nanoparticle to the surface diffusivity of atoms indicate likely movement of small particles, but a rapid decrease in the mobility with increasing size of the particle. Alternate models based on diffusion of diatomic surface species too have been proposed and employed to explain results of long-term studies of catalyst deactivation.[6] However, direct experimental confirmation of these models for particle mobility is lacking in the literature on heterogeneous catalysts.

In situ electron microscopy has been extensively used to provide direct observations of particle mobility, as pioneered by Baker[7] who suggested that the onset of mobility occurred at the Tammann temperature ($0.5 T_{\text{melting}}^{\text{bulk}}$ [K]). This is the temperature where surface atoms become mobile and this motion of atoms on the surface constitutes the mechanism for particle mobility. Previous studies show increased particle mobility with increasing temperature, but there are differences between the nature and extent of mobility that was recorded. A review by Harris[8] considering various models proposed for particle migration suggested that for Pt/Al$_2$O$_3$ at 600 °C, spherical particles ~5 nm in diameter would migrate about 540 nm in 2 h, while larger

particles, around 24 nm, would move at most a distance equal to their diameter. It is instructive to compare these predictions with direct observation of nanoparticles subjected to elevated temperatures.

We recently studied model Pt/SiO$_2$ samples[9] under 560 Pa of O$_2$ at 550 °C for up to 10 h in an environmental transmission electron microscope. The mean particle diameter was smaller than 3 nm, and the interparticle separation was about 5 nm. Over the 10 h of observation there was no significant change in the number of particles per unit area, ruling out PMC as being responsible. Similar observations were reported by Simonsen et al.[10] who found that the only coalescence events they observed were due to neighboring islands. They concluded that Pt particles (2−5 nm in diameter) did not exhibit any mobility and the mechanism of sintering was inferred to be Ostwald ripening. A similar conclusion was reached by Yoshida et al.[11] using aberration-corrected scanning transmission electron microscopy (TEM) where they were able to observe the migration of single atoms of Pt on a carbon support. Smaller particles (<100-atom clusters) of Pd/TiO$_2$ were studied by Sanders[12] using atom tracking scanning tunneling microscopy. It was found that the smallest particles executed a hopping motion but were readily pinned and stopped moving. Therefore, we infer that large scale Brownian motion of nanoparticles is unlikely to contribute to the sintering of the smallest nanoparticles in the early stages of catalyst sintering.

The Early Stage of Catalyst Sintering (Phase I)

Understanding this initial stage of sintering is important because it provides insight into the behavior of the smallest metal particles in heterogeneous catalysts which are also in many cases the most active and selective. The general shape of this dispersion versus time plot as seen in most published accounts of catalyst sintering is similar to that shown in Figure 1. The actual time frame depends on the temperature, the gas environment, and the metal under study. Using temperature programmed desorption, Beck and Carr[1] were able to study changes in dispersion at short time intervals. For aging temperatures between 700 and 900 °C, they found that Pt dispersion decreased rapidly in the first few minutes. An extensive review of the sintering of supported catalysts by Bartholomew[13] reports that the initial rapid sintering occurs within the first few hours, especially at lower temperatures. Industrial catalyst supports are heterogeneous in structure and operate at elevated temperatures in the presence of reactive gases, making it difficult to perform in situ studies. Hence, most published work relevant to industrial
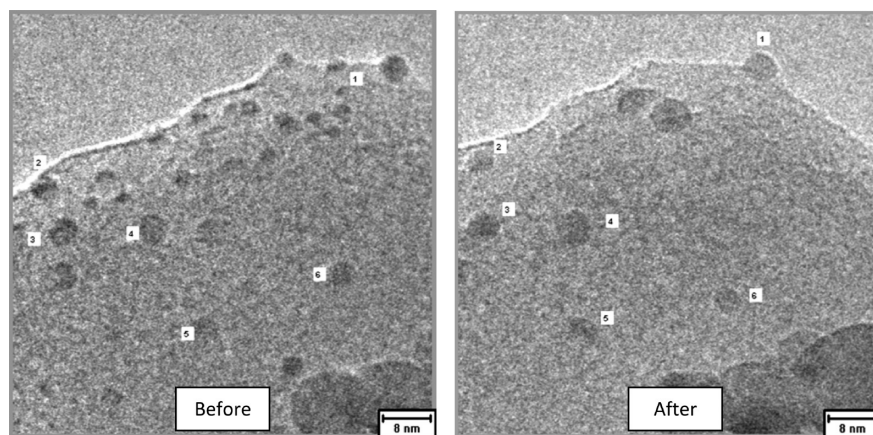
FIGURE 2. Images of Ni/MgAl$_2$O$_4$ sample before and after exposure to 1:1 H$_2$/H$_2$O at 400 Pa and 650 °C for 30 min. Many particles have disappeared over the period; the remainder are numbered for comparison. Total mass of Ni in this region was conserved (1.1 × 10^{-17} g before heating and 1.2 × 10^{-17} g after heating). Reprinted with permission from DeLaRiva.[15]

catalysts involves observations before and after catalyst aging, which is not conclusive for establishing the mechanism of sintering. With in situ capabilities now available in TEM and new microelectromechanical system (MEMS) devices,[14] it has become possible to perform sintering studies under conditions approaching those used in industrial practice, albeit limited in pressure to the 1−1000 mbar range and a time scale of hours.

Linking in situ observations of sintering over short time scales to catalyst sintering covering hundreds of hours in technical applications remains a challenge. DeLaRiva[15] studied the evolution of Ni/MgAl$_2$O$_4$ catalysts at the early stages of sintering, when the sample first reaches its operating temperature. He found that the early stages of Ni sintering were dominated by ripening of the smallest particles. Figure 2 shows an image of the Ni catalyst after reaching 650 °C and after 30 min of heating with the beam off. The small particles have all disappeared while the remaining particles (marked with numbers) have grown in size. The total mass of Ni estimated from the particle sizes is conserved, ruling out evaporation as the cause for the loss of Ni particles. These images do not directly convey the operating mechanism, since the particles could have migrated and coalesced with their neighbors. Continuous observations of the catalyst were also performed to track the events as the catalyst was heated.

Small Ni particles were found to disappear in a few seconds at the elevated temperatures (Figure 3a).[16] The time evolution of the particles was fitted to a model based on ripening and an activation energy of 264 kJ/mol was derived for the overall process of atom emission and inter-particle transport (Figure 3b) that was consistent with the

thermodynamic energies relevant for this catalyst system. Remarkably, this activation energy combined with a deterministic model for OR allowed predictions of particle size distribution after 30 min of sintering that closely matched the experimental observations.[16] This work suggests that, besides giving unambiguous mechanistic insights, direct observation of the disappearance of individual particles may also enable predictions of long-term sintering in industrial catalysts. Unfortunately, such measurements are challenging since catalyst samples are not stable when heated and the process of ripening of the smallest particles is over within seconds. Monte Carlo simulations help provide additional insight into the processes of catalyst sintering, especially the rapid initial loss of surface area.

We employed atomistic simulations of a collection of supported nanoparticles performed in a Monte Carlo scheme based on a simple 3-D lattice gas model. The details and implementation of this simple atomistic model can be found in textbooks[17] and in a recent report on the sintering of nanoparticles.[18] Reasonable physical parameters were employed for the present supported system. The advantage of such an atomistic model is that all the observed phenomena arise from thermally activated atom-hopping events and no a priori mechanism of sintering is assumed. The starting distribution of particles was taken from a TEM image of a model catalyst (such as the one shown later in Figure 9).

Snapshots of the simulation system are shown in Figure 4a. Sintering is indicated by a loss of small particles at the beginning, and eventual growth of large particles, with hardly any relative movement of particles to suggest migration. Additional evidence from tracking of individual particle sizes confirms the sintering to be caused by ripening
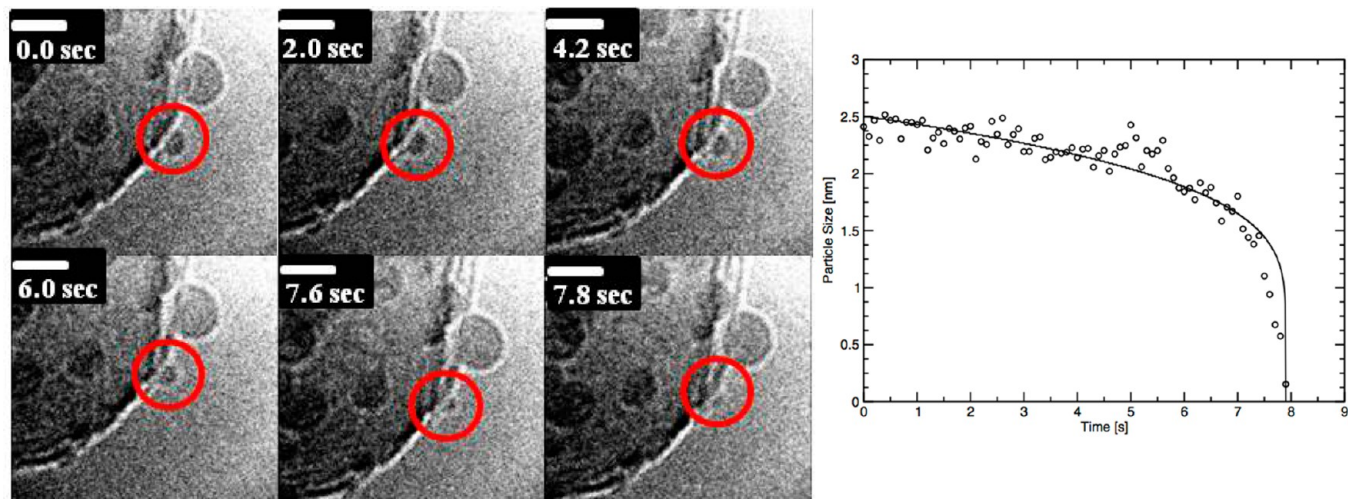
FIGURE 3. (a) Time-lapsed TEM images of $MgAl_2O_4$-supported Ni nanoparticles heated at 750 °C in 1:1 H_2/H_2O at 360 Pa. The scale bar in the images is 5 nm, and the times are indicated relative to the start of observation (which is within a few minutes after reaching the operating temperature). These images come from a movie sequence which shows the disappearance of the smallest particles. (b) The temporal evolution of the Ni nanoparticle that is circled on the left. The experimental data (circles) was fit to the equation $dr/dt = (−K_{int}/r)\exp(2\gamma\Omega/rk_bT)$ which is derived from a mean field model based on Ostwald ripening (from Challa et al.[16]).
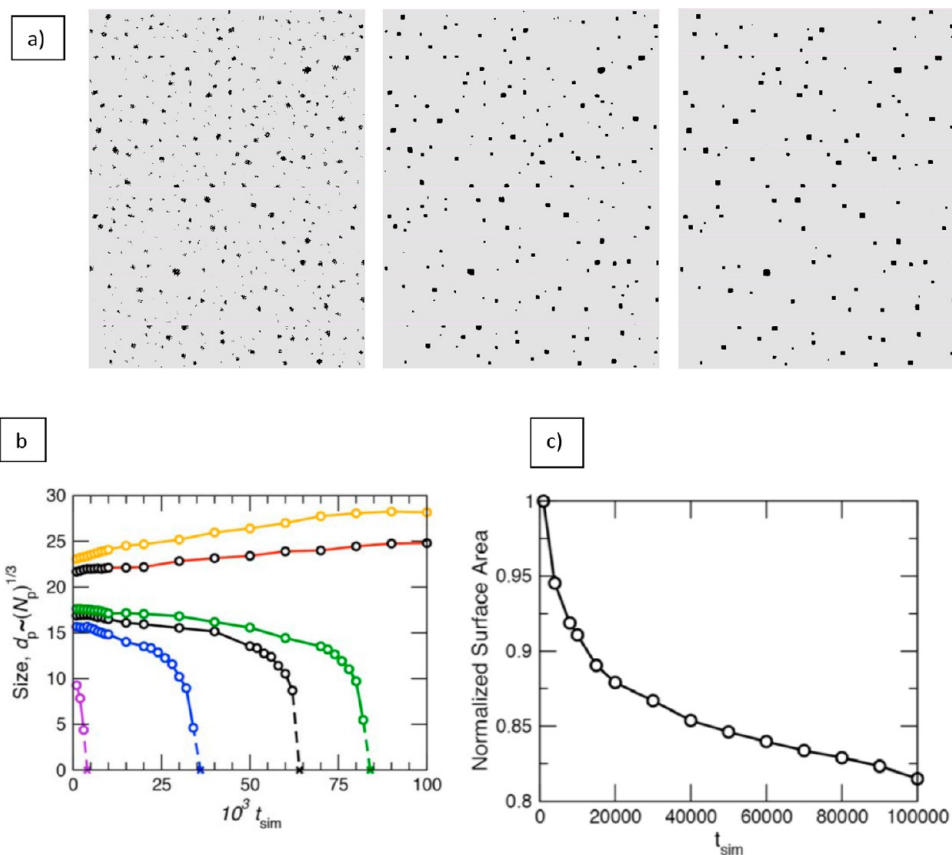

FIGURE 4. Monte Carlo (MC) simulation showing the evolution of a collection of nanoparticles: (a) Snapshots from the simulation after (left to right) 0, 10 000, and 100 000 MC steps. (b) Size evolution of six particles from the simulation. (c) The surface area of this collection of nanoparticles shows a rapid loss at short times, followed by a more gradual change at long times, but there is no change in mechanism.

(Figure 4b). An almost uniform rate of decrease in size of small particles is observed initially. This rate accelerates when the particles become smaller than a critical size, as a consequence of the enhancement of vapor pressure due to
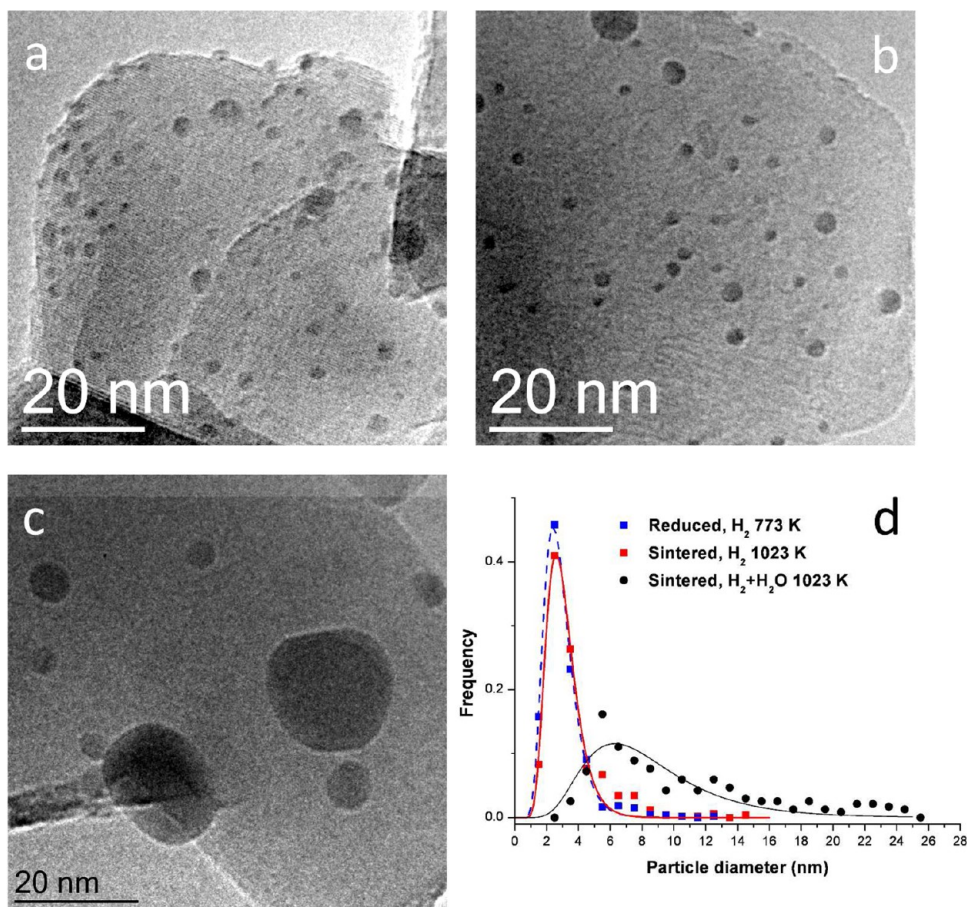
FIGURE 5. TEM images of a Ni/MgAl$_2$O$_4$ catalyst (a) after reduction in 300 Pa H$_2$ at 500 °C; (b) after sintering for 5 h in 200 Pa H$_2$ at 750 °C; (c) after sintering for 5 h in 200 Pa H$_2$ and 200 Pa H$_2$O at 750 °C;(d) particle size distributions for the three samples. These images show that the addition of water vapor plays a major role on the rate of sintering of Ni in these catalysts. Adapted from Hansen.[21]

the small radius of curvature (Gibbs–Thomson effect) for these particles. The growth of the larger particles is steady and slow, as might be associated with incorporation of adatoms into these particles. No jumps in their sizes are noted that might be associated with coalescence. The coarsening of particles being described herein is qualitatively similar to that observed experimentally (decaying particles) in Figures 2 and 3, as well as to recent literature on nanoparticle ripening.[10,16]

Additional analysis indicates only localized random motion of the particles, with displacements much less than their diameter during the entire simulation. The loss of surface area (Figure 4c) seen at the initial stages of catalyst sintering is caused by the disappearance of the small particles and the growth in size of the larger particles. It is also worth noting that surface free energy increases considerably for particles smaller than 3–5 nm and the concept of a fixed surface tension may not be applicable.[19] This could further accelerate the loss of the smallest particles, causing an enhanced decline in catalyst surface area at the early stages of catalyst sintering.

The Intermediate Stage of Catalyst Sintering (Phase II)

As the catalyst is aged, the rate of decline in catalyst surface area slows down. This is a general observation of many experimental studies using a variety of techniques.[13,20] In industrial practice when a new catalyst is brought on stream, a process called "degreening" is sometimes used (essentially a controlled sintering step) to achieve stable performance. Hansen[21] studied this stage of catalyst sintering by performing in situ measurements of Ni nanoparticles on low surface area MgAl$_2$O$_4$ supports.[22] The samples were reduced at 500 °C in the microscope and then sintered in 1:1 or 1:9 H$_2$/H$_2$O at 650 or 750 °C, respectively, in situ over a 5 h period without exposure to the electron beam. The initial samples had a log-normal-like particle size distribution with an average size of 3.2 nm and a standard deviation of 0.2. It was found that treatment in pure H$_2$ at temperatures up to 750 °C caused very little further change in the particle size (Figure 5). Also, very little sintering was observed at 650 °C in
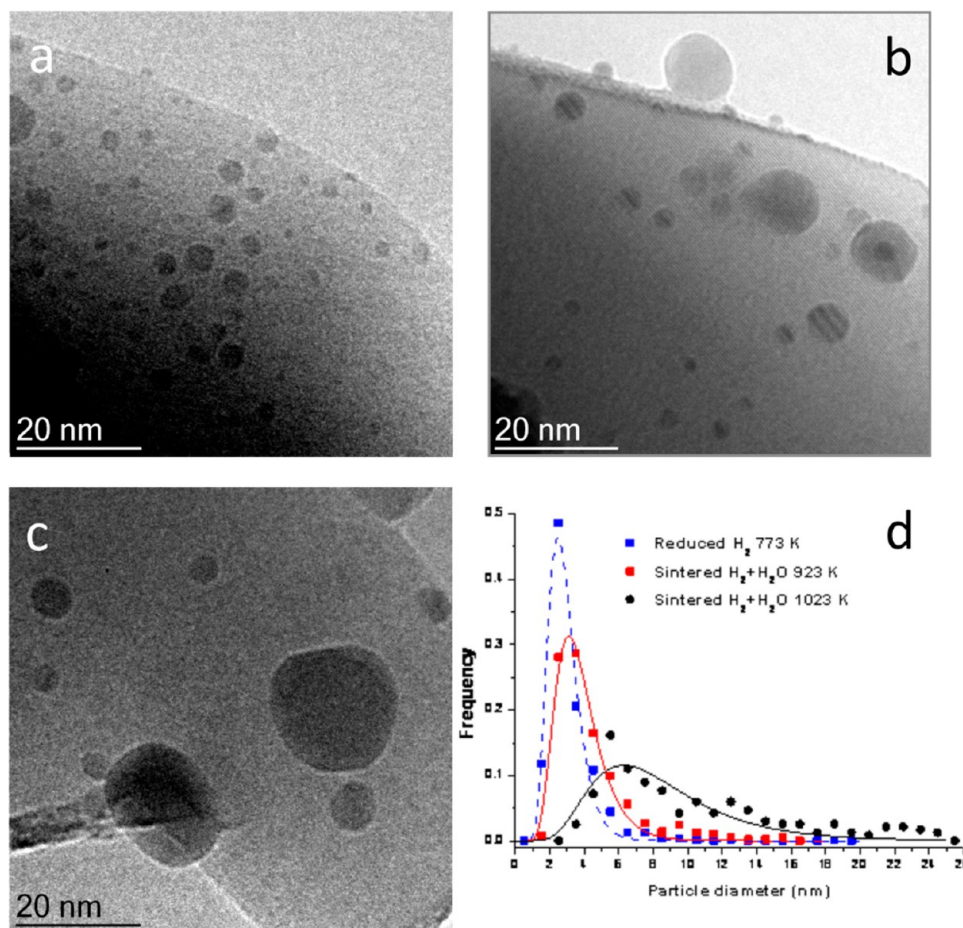
FIGURE 6. TEM images of a Ni/MgAl$_2$O$_4$ sample (a) after reduction in 300 Pa H$_2$ at 500 °C; (b) after sintering for 5 h in 200 Pa H$_2$ and 200 Pa H$_2$O at 650 °C; (c) after sintering for 5 h in 200 Pa H$_2$ and 200 Pa H$_2$O at 750 °C; (d) particle size distributions for the three cases. We can see the influence of temperature is quite significant on the rates of Ni sintering. Adapted from Hansen.[21]

1:1 H$_2$/H$_2$O after 5 h (see Figure 6). However, in the 1:1 H$_2$/H$_2$O mixture at 750 °C, the average particle size grew to 10 nm with a broad distribution. These longer term heat treatments clearly show significant particle growth in the presence of water vapor. In each case the PSDs developed a tail on the right and fit the log-normal distribution very well. Under the harshest conditions (1:1 H$_2$/H$_2$O at 750 °C), particles larger than 20 nm were observed.

While the overall rate of sintering had slowed down, there was significant change over the 5 h of observations. To determine the mechanism of sintering and the behavior of the metal nanoparticles under these conditions, the experiments were repeated while the particles were observed under the electron beam. The observations indicated that the particles were stationary, with little noticeable random motion. Whenever migration occurred, it was due to particles around 10 nm or larger. When these migrating particles encountered other particles on the support, they tended to coalesce and become spheroidal within one image frame (500 ms). The migration often occurred along steps on the substrate surface and was discontinuous. Figure 7 shows the frames captured from an image sequence where the original position of the particles is indicated in white. At 13 s, particle I coalesces with the small particle adjacent to it. Then particle II migrates along the step and coalesces with smaller stable particles along this edge (the edge is noticeable in the image at 13 s). The center of mass of the particle has moved one particle diameter, but the entire migration is longer as the particle travels along the step. Particle III translates approximately one particle diameter to the left at 25 s. During the entire sequence, particle IV remains immobile. By following the sequence of frames we can see that it is the large particles that move, and when the particles come close to each other, coalescence occurs following a mechanism similar to that reported by Yang et al.[23]

The contribution of these coalescence events to the overall sintering rate has not yet been determined. However, we
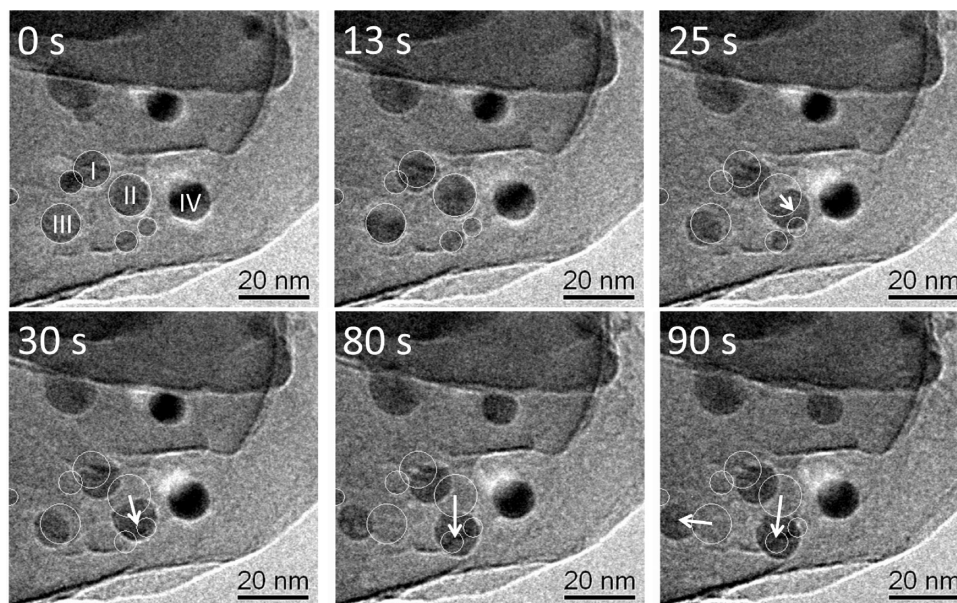
FIGURE 7. TEM images of Ni/MgAl$_2$O$_4$ catalyst shown in Figures 5 and 6. This is an image sequence acquired in 200 Pa H$_2$O and 200 Pa H$_2$ at 750 °C. Individual frames have been aligned to make it easier to see the motion of individual nanoparticles and to allow us to track these particles. The frames are acquired at 0, 13, 25, 30, 80, and 90 s. The white circles indicate the initial positions of the particles and four particles that survived at the end of the treatment are indicated with numbers I−IV. Arrows show the particle mobility seen in the next frame. The image sequence shows that the larger particles are more mobile than the smaller particles, and the particles appear to nucleate preferentially at steps on the support. Adapted from Hansen.[21]

can confirm that many hours of recording image sequences only showed immobile particles, observations such as those reported in Figure 7 were rare. It might be speculated that the long tail in the PSD (Figures 5 and 6) could be the result of particle migration and coalescence. However, recent in situ experiments performed with Pt and Pd catalysts[9] showed that anomalous growth patterns, where some particles grow significantly larger than the mean, occurred under conditions where the particles were immobile and the only operative mechanism was Ostwald ripening.

The original formulation of the mechanism of sintering by coalescence assumes diffusive particle migration. Other mechanisms are also likely, and possibly significant, such as attractive migration and coalescence,[9,23] nondiffusive migration along edges (noted above) with possible collisions, or simple coalescence of particles without any migration when the particles are close enough to be either touching or having an overlapping diffusive field of adatom species. It has also been observed that under oxidizing conditions, metal nanoparticles (Ni, Fe, Cu, Ag, Pd, Pt, Co) can spread on the support surface (alumina, silica, carbon), which can lead to overlap of neighboring particles and eventual particle coalescence.[24−27] Such spreading has been attributed to increased wetting by the oxidized metal.[25] The Ni nanoparticles under steam reforming conditions in the present study

are observed under reducing conditions and exhibit dewetting as the particles grow in size; hence, it is unlikely that oxidation could lead to the observed events.

Long-Term Catalyst Sintering (Phase III)

Most academic studies are performed over a few hours and come to the conclusion that quasi-equilibrium is reached, and the catalyst stops sintering. This seems more likely at lower temperatures, but assuming that the mechanism is Ostwald ripening, the process of sintering, at high temperatures, may never stop completely; it may just slow down enough to be undetectable over short periods of time. The data[28] shown in Figure 1a suggests that sintering slows down as one approaches 100 h of aging. But when plotted on a log scale, it is clear from Figure 1b that the process of sintering has not ceased. Longer term aging studies on Pd/alumina combustion catalysts[29] at 900 °C and 9.5 bar pressure found that the sintering process continued over ~4000 h of observation. The particle dispersion could be modeled by a power law expression (see the equation in Figure 1) with an exponent of $n = 3$. The data in Figure 1 obtained at 900 °C and 1 bar was fitted with an exponent of $n = 2$. Knowledge of these exponents from such aging studies is important for predicting the long-term performance of combustion catalysts. However, the dispersion
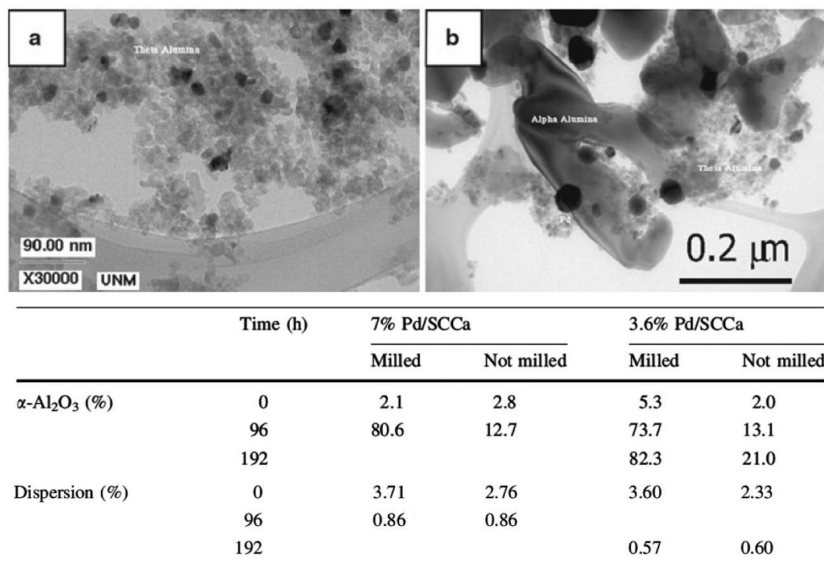
	Time (h)	7% Pd/SCCa		3.6% Pd/SCCa	
		Milled	Not milled	Milled	Not milled
α-Al$_2$O$_3$ (%)	0	2.1	2.8	5.3	2.0
	96	80.6	12.7	73.7	13.1
	192			82.3	21.0
Dispersion (%)	0	3.71	2.76	3.60	2.33
	96	0.86	0.86		
	192			0.57	0.60

FIGURE 8. TEM images of a 7% Pd/Al$_2$O$_3$ heated at 900 °C in 10% H$_2$O/N$_2$ for (a) 0 h and (b) 96 h. The support Al$_2$O$_3$ is seen to change from theta to alpha phase over 96 h. The table shows the % α-alumina determined by X-ray diffraction and the dispersion of Pd, for catalysts that were milled and not milled. Milling accelerates the phase transformation, causing a loss of surface area, but has minimal impact on the dispersion of Pd after aging. (Adapted from Xu et al.,[30] *Topics in Catalysis*, with permission.)

determined from sintering studies at high temperatures and long times does not support the hypothesis that equilibrium dispersion is ever reached. Nevertheless, depending on the operating conditions, it may be possible to slow down sintering to allow operation of industrial catalysts for thousands of hours.

At high temperatures, other parasitic phenomena, such as support sintering, also become important. For instance, at 900 °C, we have already exceeded the Tammann temperature for alumina. The alumina transforms from a high surface area transitional alumina into low surface area α-alumina. The process of phase transformation could be slowed down by skipping the step of ball milling traditionally used in automotive catalyst preparation.[30] To our surprise, we learned that preventing surface area loss was insufficient to prevent sintering, as shown in Figure 8. Since all supports lose surface area during sintering, it was also important to perform experiments with supports that are in their thermodynamically stable state and that, hence, would not lose any surface area. We studied various model catalyst supports: single crystals of sapphire, quartz and yttria-stabilized zirconia, with similar loadings of Pd and subjected to long-term aging at 900 °C in N$_2$. As shown in Figure 9, we found that the final particle size was significantly different, with ZrO$_2$ yielding the smallest average particle size. We conclude that support chemistry plays a major role in influencing the rate of sintering in these samples.

Summary

We have examined recent results that shed light on the mechanism of catalyst sintering. We have divided the sintering of catalysts into three phases. The first phase shows rapid decay of surface area and appears to be dominated by Ostwald ripening. The rapid loss in surface area is caused by the disappearance of the smallest particles, as seen both via in situ TEM and Monte Carlo simulations. The results show that Brownian-like motion of nanoparticles is not a dominant process, and may not play a significant role at moderate temperatures (up to 750 °C) on industrially relevant supports. In the later phases, when particles have grown larger, we do see evidence of particle coalescence, usually at higher temperatures and only when nanoparticles are in close proximity. Sintering slows down as particles grow in size and interparticle separation increases.

One approach to control sintering relies on anchoring metal nanoparticles within a porous support. The results in the literature show improved catalytic performance when compared with the same metal deposited on conventional supports.[31−33] However, if particle migration was the mechanism of sintering for the smallest particles, one would expect that particle growth would cease when the nanoparticle size approaches the pore diameter. Closer examination of the data shows that even when nanoparticles stay inside the pores after high temperature treatments, the metal particle sizes grow larger than the pore size.[31−33] This is a
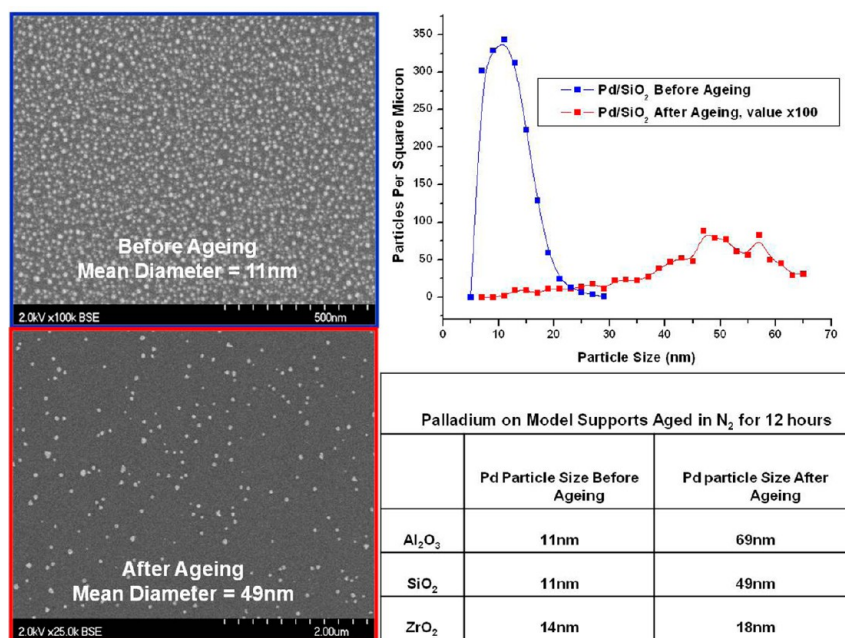
FIGURE 9. SEM images of Pd/SiO₂ model catalyst heated to 900 °C in N₂ at 70 000 Pa for 12 h. The particle size distribution shows a significant increase in particle size due to sintering. Similar experiments were performed on other model supports as shown in the table. It is clear that the support plays a significant role in controlling the growth in particle size (from DeLaRiva[15]).

clear indication that Ostwald ripening must be involved, since transfer of atomic species can continue even when the particle size exceeds the pore size. The improved catalytic performance in these catalysts must result from confining the particles within the porous structure. The lack of pore connectivity may slow the overall rate of sintering and a second benefit is improved metal−support contact within the pore structure. This is likely the mechanism leading to the improved stability shown recently for Cu in mesoporous silica.[34]

Another approach proposed in the literature involves the addition of a second component (as in a bimetallic[31]) or an oxide phase that is applied as an overcoat,[35] or in the form of a dispersed phase.[36] An overcoat of alumina on Pd was shown to lead to improved performance, which was attributed to blocking the edge and corner sites from where atoms would be emitted in a ripening process. Adding small amounts of BaO to alumina allowed redispersion of Ir catalysts during oxidizing conditions.[36] Small amounts of titania on silica,[37] and of silica on titania,[38] led to improved stability of Au nanoparticles. All of these improvements can be related to changes in the composition of the nanoparticles or changes in support surface structure, morphology and chemistry, which could alter the rates of atom emission and transport on the support. We agree with the sentiment voiced in a recent review, that the most important

mechanism of sintering is the movement of atoms rather than particles.[39] We hope that this account of the mechanisms of nanoparticle sintering will help future designs of catalysts that provide improved long-term performance in heterogeneous catalysts.

BIOGRAPHICAL INFORMATION

Thomas W. Hansen received his Ph.D. in 2006 from the Technical University of Denmark. He did postdoctoral research at the Fritz Haber Institute in Berlin, Germany. Since 2008 he is a senior researcher at the Center for Electron Nanoscopy, Technical University of Denmark.

Andrew T. DeLaRiva received his Ph.D. in 2010 from the University of New Mexico. He is currently a postdoctoral researcher in the Center for Microengineered Materials at the University of New Mexico.

Sivakumar R. Challa received his Ph.D. in 2001 from the University of Pittsburgh. His current research is focused on using computational models in the field of hydrodynamics and

thermodynamics of nanomaterials for energy and catalytic systems. He is currently a research professor at the University of New Mexico.

Abhaya K. Datye received his Ph.D. in 1984 from the University of Michigan. Since then he has served on the faculty of the University of New Mexico where his current title is Distinguished Regents Professor of Chemical & Nuclear Engineering. His research interests are in the application of electron microscopy for the study of catalysts, generation of H_2 from steam reforming and the design of catalysts for improved hydrothermal stability for aqueous phase and high temperature reactions.

FOOTNOTES

*To whom correspondence should be addressed. E-mail: datye@unm.edu.
The authors declare no competing financial interest.

REFERENCES

1 Beck, D. D.; Carr, C. J. A study of Thermal Aging of Pt/Al₂O₃ Using Temperature-Programmed Desorption Spectroscopy. *J. Catal.* **1988**, *110*, 285–297.

2 Wynblatt, P.; Gjostein, N. A. Supported Metal Crystallites. *Prog. Solid State Chem.* **1975**, *9*, 21–58.

3 Granqvist, C. G.; Buhrman, R. A. Statistical-Model for Coalescence of Islands in Discontinuous Films. *Appl. Phys. Lett.* **1975**, *27*, 693–694.

4 Datye, A. K.; Xu, Q.; Kharas, K. C.; McCarty, J. M. Particle Size Distributions in Heterogeneous Catalysts: What do they tell us about the Sintering Mechanism? *Catal. Today.* **2006**, *111*, 59–67.

5 Fuentes, G. A.; Salinas-Rodriguez, E. Realistic Particle Size Distributions during Sintering by Ostwald Ripening. *Stud. Surf. Sci. Catal.* **2001**, *139*, 503.

6 Sehested, J. Sintering of Nickel Steam Reforming Catalysts. *J. Catal.* **2003**, *217*, 417–426.

7 Baker, R. T. K. The Relationship between Particle Motion on a Graphite Surface and Tammann Temperature. *J. Catal.* **1982**, *78*, 473–476.

8 Harris, P. J. F. Growth and Structure of Supported Metal Catalyst Particles. *Int. Mater. Rev.* **1995**, *40*, 97–115.

9 Benavidez, A. D.; Kovarik, L.; Genc, A.; Agrawal, N.; Larsson, E. M.; Hansen, T. W.; Karim, A. M.; Datye, A. K. Environmental Transmission Electron Microscopy Study of the Origins of Anomalous Particle Size Distributions in Supported Metal Catalysts. *ACS Catal.* **2012**, *2*, 2349–2356.

10 Simonsen, S. B.; Chorkendorff, I.; Dahl, S.; Skoglundh, M.; Sehested, J.; Helveg, S. Direct Observations of Oxygen-induced Platinum Nanoparticle Ripening Studied by In Situ TEM. *J. Am. Chem. Soc.* **2010**, *132*, 7968–7975.

11 Yoshida, K.; Bright, A.; Tanaka, N. Direct Observation of the Initial Process of Ostwald Ripening using Spherical Aberration-Corrected Transmission Electron Microscopy. *J. Electron Microsc.* **2012**, *61*, 99–103.

12 Sanders, L. M. Diffusion of Three-Dimensional Metal Particles on an Oxide Surface: Implications for the Sintering of Heterogeneous Catalysts. Ph.D. Dissertation, University of New Mexico, 2003.

13 Bartholomew, C. H. Sintering Kinetics of Supported Metals: New Perspectives from a Unifying GPLE Treatment. *Appl. Catal., A* **1993**, *107*, 1–57.

14 Creemer, J. F.; Helveg, S.; Kooyman, P. J.; Molenbroek, A. M.; Zandbergen, H. W.; Sarro, P. M. A MEMS Reactor for Atomic-Scale Microscopy of Nanomaterials Under Industrially Relevant Conditions. *J. Microelectromech. Syst.* **2010**, *19*, 254–264.

15 DeLaRiva, A. Sintering of Ni/MgAl₂O₄ Catalyst via In-Situ TEM. Ph.D. Dissertation, University of New Mexico, 2010.

16 Challa, S. R.; Delariva, A. T.; Hansen, T. W.; Helveg, S.; Sehested, J.; Hansen, P. L.; Garzon, F.; Datye, A. K. Relating Rates of Catalyst Sintering to the Disappearance of Individual Nanoparticles during Ostwald Ripening. *J. Am. Chem. Soc.* **2011**, *133*, 20672–20675.

17 Binder, K.; Heermann, D. W. *Monte Carlo Simulations in Statistical Physics*, 3rd ed.; Springer-Verlag: Berlin, 1997.

18 Challa, S. R.; Song, Y. J.; Shelnutt, J. A.; Miller, J. E.; van Swol, F. Evolution of Dendritic Nanosheets into Durable Holey Sheets: A Lattice Gas Simulation Study. *J. Porphyrins Phthalocyanines* **2011**, *15*, 449–458.

19 Campbell, C. T.; Parker, S. C.; Starr, D. E. The Effect of Size-Dependent Nanoparticle Energetics on Catalyst Sintering. *Science* **2002**, *298*, 811–814.

20 Sehested, J.; Carlsson, A.; Janssens, T.; Hansen, P.; Datye, A. Sintering of Nickel Steam-Reforming Catalysts on Mg Al₂O₄ Spinel Supports. *J. Catal.* **2001**, *197*, 200–209.

21 Hansen, T. W. Sintering and Particle Dynamics in Supported Metal Catalysts. Ph.D. Dissertation, Technical University of Denmark, 2006.

22 Hansen, T. W.; Wagner, J. B.; Hansen, P. L.; Dahl, S.; Topsoe, H.; Jacobsen, C. J. H. Atomic-Resolution In Situ Transmission Electron Microscopy of a Promoter of a Heterogeneous Catalyst. *Science* **2001**, *294*, 1508–1510.

23 Yang, W. C.; Zeman, M.; Ade, H.; Nemanich, R. J. Attractive Migration and Coalescence: A Significant Process in the Coarsening of TiSi₂ Islands on the Si(111) Surface. *Phys. Rev. Lett.* **2003**, *90*, 136102.

24 Chen, J. J.; Ruckenstein, E. Role of Interfacial Phenomena in the Behavior of Alumina-Supported Palladium Crystallites in Oxygen. *J. Phys. Chem.* **1981**, *85*, 1606–1612.

25 Ruckenstein, E.; Lee, S. H. Redispersion and Migration of Ni Supported on Alumina. *J. Catal.* **1984**, *86*, 457–464.

26 Gai, P. L.; Smith, B. C.; Owen, G. Bulk Diffusion of Metal Particles on Ceramic Substrates. *Nature* **1990**, *348*, 430–432.

27 Kliewer, C. E.; Kiss, G.; DeMartin, G. J. Ex Situ Transmission Electron Microscopy: A Fixed-Bed Reactor Approach. *Microsc. Microanal.* **2006**, *12*, 135–144.

28 Xu, Q.; Kharas, K. C.; Croley, B. J.; Datye, A. K. The Sintering of Supported Pd Automotive Catalysts. *ChemCatChem* **2011**, *3*, 1004–1014.

29 McCarty, J. G.; Malukhin, G.; Poojary, D. M.; Datye, A. K.; Xu, Q. Thermal Coarsening of Supported Palladium Combustion Catalysts. *J. Phys. Chem. B* **2005**, *109*, 2387–2391.

30 Xu, Q.; Kharas, K.; Croley, B.; Datye, A. The Contribution of Alumina Phase Transformations to the Sintering of Pd Automotive Catalysts. *Top. Catal.* **2012**, *55*, 78–83.

31 Cao, A.; Lu, R.; Veser, G. Stabilizing Metal Nanoparticles for Heterogeneous Catalysis. *Phys. Chem. Chem. Phys.* **2010**, *12*, 13499–13510.

32 Tavasoli, A.; Trepanier, M.; Dalai, A. K.; Abatzoglou, N. Effects of Confinement in Carbon Nanotubes on the Activity, Selectivity, and Lifetime of Fischer—Tropsch Co/Carbon Nanotube Catalysts. *J. Chem. Eng. Data* **2010**, *55*, 2757–2763.

33 Bore, M. T.; Pham, H. N.; Switzer, E. E.; Ward, T. L.; Fukuoka, A.; Datye, A. K. The Role of Pore Size and Structure on the Thermal Stability of Gold Nanoparticles within Mesoporous Silica. *J. Phys. Chem. B* **2005**, *109*, 2873–2880.

34 Prieto, G.; Zecevic, J.; Friedrich, H.; de Jong, K. P.; de Jongh, P. E. Towards Stable Catalysts by Controlling Collective Properties of Supported Metal Nanoparticles. *Nat. Mater.* **2013**, *12*, 34–39.

35 Lu, J. L.; Fu, B. S.; Kung, M. C.; Xiao, G. M.; Elam, J. W.; Kung, H. H.; Stair, P. C. Coking- and Sintering-Resistant Palladium Catalysts Achieved Through Atomic Layer Deposition. *Science* **2012**, *335*, 1205–1208.

36 McVicker, G. B.; Garten, R. L.; Baker, R. T. K. Surface-area Stabilization of Ir-Al₂O₃ Catalysts by CaO, SrO, and BaO under Oxygen Atmospheres - Implications on Mechanism of Catalyst Sintering and Re-dispersion. *J. Catal.* **1978**, *54*, 129–142.

37 Gabaldon, J. P.; Bore, M.; Datye, A. K. Mesoporous Silica Supports for Improved Thermal Stability in Supported Au Catalysts. *Top. Catal.* **2007**, *44*, 253–262.

38 Rashkeev, S. N.; Dai, S.; Overbury, S. H. Modification of Au/TiO₂ Nanosystems by SiO₂ Monolayers: Toward the Control of the Catalyst Activity and Stability. *J. Phys. Chem. C* **2010**, *114*, 2996–3002.

39 Moulijn, J. A.; van Diepen, A. E.; Kapteijn, F. Catalyst deactivation: Is It Predictable? What to Do? *Appl. Catal., A* **2001**, *212*, 3–16.